Molecules incorporating a benzothiazole core scaffold inhibit the N-myristoyltransferase of Plasmodium falciparum

Paul W Bowyer, Ruwani S Gunaratne, Munira Grainger, Chrislaine Withers-Martinez, Sasala R Wickramsinghe, Edward W Tate, Robin J Leatherbarrow, Katherine A Brown, Anthony A Holder, Deborah F Smith

Molecules incorporating a benzothiazole core scaffold inhibit the *N*-myristoyltransferase of *Plasmodium falciparum*

Paul W. BOWYER[*,†,‡], Ruwani S. GUNARATNE[§], Munira GRAINGER[§], Chrislaine WITHERS-MARTINEZ[§], Sasala R. WICKRAMSINGHE[‡], Edward W. TATE[‡], Robin J. LEATHERBARROW[‡], Katherine A. BROWN[†], Anthony A. HOLDER[§], Deborah F. SMITH[*,†,‖]

Wellcome Trust Laboratories for Molecular Parasitology[*], Division of Cell and Molecular Biology, Centre for Molecular Microbiology and Infection[†], Department of Chemistry[‡], Imperial College London, London SW7 2AZ, UK.
Division of Parasitology[§], MRC National Institute for Medical Research, Mill Hill, London, NW7 1AA, UK
Immunology and Infection Unit[‖], Department of Biology/Hull York Medical School, University of York, Heslington, York YO10 5YW, UK

Current addresses:
PWB – Department of Pathology, Stanford University School of Medicine, 300 Pasteur Drive, Stanford, CA 94305-5324, USA
RSG - Department of Paediatric Oncology, The Royal Marsden NHS Foundation Trust, Downs Road, Sutton, Surrey SM2 5PT, UK

Corresponding authors:
DFS, Immunology and Infection Unit, Department of Biology/Hull York Medical School, University of York, Heslington, York YO10 5YW, UK
Phone: +44 1904 328843; Fax: +44 1904 32844; Email: dfs501@york.ac.uk
AAH, Division of Parasitology, MRC National Institute for Medical Research, Mill Hill, London NW7 1AA
Phone: +44 (0)20 8816 2175; Fax: +44 (0)20 8816 2730; Email: aholder@nimr.mrc.ac.uk

Running title: Inhibition of *Plasmodium falciparum N*-myristoyltransferase

Keywords: *Plasmodium falciparum*, *N*-myristoylation, codon optimisation, SPA, inhibition, benzothiazole.

Abbreviations: NMT, myristoyl CoA:protein *N*-myristoyltransferase; SPA, scintillation proximity assay

SUMMARY

Recombinant *N*-myristoyltransferase of *Plasmodium falciparum* (PfNMT) has been used in the development of a scintillation proximity assay (SPA) suitable for automation and high throughput screening of inhibitors against this enzyme. The ability to use the SPA has been facilitated by development of an expression and purification system which yields considerably improved quantities of soluble, active recombinant PfNMT compared to previous studies. Specifically, yields of pure protein have been increased from 12 μg L^{-1} to > 400 μg L^{-1} by use of a synthetic gene with codon usage optimised for expression in an *Escherichia coli* host. Preliminary small-scale 'piggyback' inhibitor studies using the SPA have identified a family of related molecules containing a core benzothiazole scaffold with IC_{50} values < 50 μM, which demonstrate selectivity over human NMT1. Two of these compounds, when tested against cultured parasites *in vitro*, reduce parasitaemia by > 80% at 10 μM.

INTRODUCTION

Malaria is a devastating disease with an estimated 300-500 million cases and >1 million deaths per year [1]. Resistance to established anti-malarial drugs is increasing the need for the development of new compounds to combat the disease. Here we describe investigations into the *N*-myristoyltransferase of *Plasmodium falciparum* as a potential target for development of novel chemotherapeutics.

Myristoyl-CoA protein *N*-myristoyltransferase (NMT; EC 2.1.3.97) is an enzyme that catalyses the co-translational transfer [2] of the fatty acid, myristate ($C_{14:0}$), from myristoyl-CoA to the *N*-terminal glycine of target eukaryotic proteins, as well as to viral and bacterial proteins myristoylated within the host cell [3-5]. The reaction proceeds via an ordered Bi-Bi mechanism [6] in which myristoyl-CoA initially binds, followed by a putative structural rearrangement and binding of the N-terminus of the protein substrate. Myristate transfer to the *N*-terminal glycine of the protein substrate and step-wise dissociation of CoA followed by the myristoylated protein completes the reaction [7, 8].

NMT has been extensively investigated as a drug target against pathogenic fungi (reviewed in [9, 10]) and also identified as a potential target in kinetoplastid parasites [11] as well as a novel anti-cancer agent [12-15]. Genetic analyses of NMT have shown recessive lethality in *Saccharomyces cerevisiae*, while NMT is an essential gene in *Candida albicans*, *Cryptococcus neoformans* [16, 17], *Trypanosoma brucei* and *Leishmania major* [18]. Comparative analyses of human and fungal NMTs have shown that the peptide pocket is less well conserved than the myristoyl-CoA binding site [19]. Although myristoyl-CoA analogues have been shown to have anti-viral activity [20], selective inhibition can be best achieved by targeting the peptide-binding pocket. For example, inhibitors of the NMT peptide-binding pocket in pathogenic fungi are capable of inhibiting *C. albicans* NMT (CaNMT) with IC_{50} values in the nanomolar range [10, 21-23] and show >1000-fold selectivity over human NMTs. There are two NMT genes in humans, (*Homo sapiens N*-myristoyltransferase 1 and 2 [24, 25]). Their protein products, HsNMT1 and HsNMT2, show 73% identity to each other and 40% - 50% identity with the NMTs of *C. albicans*, *T. brucei* and *P. falciparum*. Investigations into inhibitors of HsNMT1 have identified a family of compounds based around a cyclohexyl-octahydro-pyrrolo[1,2-a] pyrazine scaffold with IC_{50} values in the low micromolar range [26].

NMT activity has also been studied in kinetoplastid parasites. Establishment of robust expression and purification protocols for recombinant forms of *T. brucei* NMT (TbNMT) and *L. major* NMT (LmNMT) in *Escherichia coli* has enabled compounds to be tested for inhibition of these enzymes, in a piggy-back approach [11], leading to identification of inhibitors selective for TbNMT [27]. In comparison, only low expression of recombinant *P. falciparum* NMT (PfNMT) (12 $\mu g\ L^{-1}$) has been reported to date [28] and this has limited the initiation of similar studies. However, like TbNMT and LmNMT, PfNMT has considerable potential as an antimalarial drug

target. PfNMT is encoded as a single copy gene (PF14_0127) with detectable mRNA in the asexual blood stage forms and the recombinant protein shows differential inhibition profiles compared to HsNMT1 [25]. A range of *N*-myristoylated substrates from *P. falciparum* (including GAP (PFL1090w) [29], GRASP, (PF10_0168) [30] and CDPK (PFB0815w) [31]) have been identified biochemically. In addition, more than 40 potential substrates with a high likelihood of being *N*-myristoylated have been identified by bioinformatic and biochemical predictions; these include ADP Ribosylation Factors, CDPKs and several PfEMP1s [32]. The presence of these known and predicted substrates of PfNMT suggests that inhibition of this enzyme would disrupt a range of biochemical pathways, ultimately resulting in loss of parasite viability.

To further study the potential of PfNMT as a drug target, we describe here the improved expression and purification of a recombinant form of the enzyme from *E. coli*, utilising a synthetic codon-optimised *PfNMT* gene. Furthermore, we also report the development of a scintillation proximity assay (SPA) amenable to high-throughput screening and demonstrate how this assay has been used for the identification of inhibitors showing activity against both recombinant PfNMT and the cultured asexual stages of *P. falciparum*.

METHODS

Codon optimisation for PfNMT expression in *E. coli*

The codon usage in the native *PfNMT* gene was modified to give a new synthetic gene with codons optimal for expression in *E. coli*. The synthetic gene was designed with the help of a Perl script program, CODOP, that allows codon optimisation for a given host organism [33]. The program allowed the insertion of desired restriction sites and generated 40-mer oligonucleotides for both strands of the gene with a melting temperature for each of the 20 nucleotide overlaps of around 60 ^{o}C. The oligonucleotides were checked for presence of repeats, stem-loops and overlaps using the Genetics Computer Group software package (version 8-Unix). A total of 60 oligonucleotides were obtained; the two end fragments were longer (49 and 61 nucleotides) to include the restriction sites *Bam*HI and *Eco*RI for subsequent subcloning. The sequence was then assembled and amplified as described [34], achieving a reduction in AT content from 73% to 60%. The amplified fragment was cloned into the vector pTrcHisA (Invitrogen) and the sequence confirmed. The resulting plasmid, pTrcNMT, was transformed into *E. coli* BL21(*DE3*)pLysS for expression studies.

Overexpression and purification of recombinant PfNMT, HsNMT1 and CaNMT

Expression of N-terminally His-tagged PfNMT from pTrcNMT was induced in *E. coli* BL21(*DE3*)pLysS in the presence of 100 μg ml^{-1} ampicillin. A single bacterial colony was grown for 16 h in L-broth (LB) at 37 ^{o}C with shaking at 220 r.p.m. Inoculation (1:20) of fresh LB was followed by growth at 37 °C, 220 r.p.m. to an OD_{600} of 0.6. The culture temperature was reduced to 30 °C before induction with 0.1 mM IPTG (isopropyl β-D-thiogalactoside) and growth at 30 °C for 4-5 h. Cells were pelleted by centrifugation (14000 *g*, 10 min) and resuspended in cell lysis buffer (300 mM NaCl, 50 mM NaH_2PO_4, 5 mM DTT, 20 mM imidazole, pH 7.0 supplemented with 2% v/v Triton X-100) in the presence of EDTA-free mini complete protease inhibitors (Roche). Cells were then treated with lysozyme (1 mg ml^{-1}, 30 min on ice), followed by sonication on ice (three rounds of 2 x 10 s pulses at 15 W). The soluble fraction was isolated by two rounds of centrifugation (40000 *g*, 4 °C) and recombinant His-tagged protein recovered by immobilized metal affinity (IMAC) resin using Ni-Sepharose (GE Healthcare) according to the manufacturer's protocol, with elution by 500 mM imidazole.

Fractions containing NMT activity were pooled and buffer exchanged into 50 mM NaCl, 100 mM NaH_2PO_4, 5 mM DTT, pH 7.0 by sequential concentration and dilution (3 rounds on Centricon YM-30 spin columns; Millipore) to a final volume of 2 mL. The sample was filtered (0.44 μM filter) before applying to a Sephacryl S-100 column connected to an $AKTA_{FPLC}$ system (GE Healthcare), maintained at 4 °C, using at a flow rate of 0.2 mL min^{-1}. Fractions containing NMT activity were pooled, diluted to 50 mL in 50 mM NaH_2PO_4, 5 mM DTT, pH 6.5 and applied using a 50 mL superloop to a ReSOURCE S strong cation exchange column. Elution was

conducted using a 0 – 1 M NaCl gradient in the same buffer at a flow rate of 2 mL min^{-1}. Products were analysed by SDS-PAGE and the identity of the major band (*ca.* 50 kDa) confirmed as PfNMT by MALDI-TOF mass spectrometry.

Plasmids encoding HsNMT1 (in pET20b) and CaNMT (in pET11c), were provided by Pfizer (Sandwich, Kent, UK). Recombinant forms of these proteins were expressed in *E. coli* BL21(*DE3*)pLysS as above and cells lysed in 50 mM TrisHCl, 2 mM EGTA, pH 8.6 (HsNMT) or 20 mM TrisHCl, 1 mM DTT pH 7.4 (CaNMT). For both soluble lysates, NMT activity was enriched by anion exchange using a 30 mL DEAE Sepharose column, with elution over a 0 – 1 M NaCl gradient at a flow rate of 3 mL min^{-1}. All NMTs were stored in 25% glycerol at -20 ºC.

NMT activity and inhibition assay

Biontinylated peptide substrates based on the N-terminal sequence of *P. falciparum* ADP ribosylation factor 1 (PfARF1) were prepared by solid phase peptide synthesis (SPPS) using standard Fmoc/^{t}Bu chemistry [35]. The peptides GLYVSRLFNRLFQKK(Biotin)-NH_2 and GLYVSRLFNRLFQK(Biotin)-NH_2 (PfARFlong and PfARFshort respectively) were synthesized, purified by reverse phase HPLC using a C18 column (Waters) and freeze dried. Controls in which the N-terminal glycine was replaced by alanine were also prepared. These substrates were used to develop a scintillation proximity assay (SPA) for NMT activity amenable to a 96-well plate format. [^{3}H]-myristoyl-CoA (GE Healthcare) was supplemented with unlabelled myristoyl-CoA (Sigma) to achieve required specific activities (generally 8 Ci/mmol). Recombinant enzyme was prepared as described above.

100 µL reactions contained equal volumes of buffer (or inhibitor), recombinant NMT, 125 nM [^{3}H]-myristoyl CoA (8 Ci $mmol^{-1}$) and 125 nM biotinylated peptide substrate. All solutions were prepared using assay buffer (30 mM Tris, 0.5 mM EGTA, 0.5 mM EDTA, 2.5 mM DTT adjusted to pH 7.4 with HCl, 0.1% Triton X-100). DMSO was present at a final concentration of 1% (v/v). The reactions were initiated by addition of peptide substrate after a 5 min pre-incubation and allowed to proceed for 30 min at 37 ºC before termination with 100 µL of stop solution (50 mg/ml SPA beads in PBS/0.05% sodium azide diluted 50 times with 1:1 0.2 M phosphoric acid buffered to pH 4.0 with NaOH and 1.5 M $MgCl_2$). The plate was then sealed and beads allowed to settle for > 8 h before scintillation counting using a Chameleon plate reader (Hidex, Finland).

K_M determinations

The apparent K_M for the myristoyl-CoA binding of PfNMT was determined by varying the myristoyl-CoA concentration from 0 - 500 nM (8 Ci $mmol^{-1}$) at a constant peptide concentration (500 nM) and enzyme concentration using the scintillation proximity assay. Similarly the apparent K_M for the biotinylated peptide substrates was determined over the range 78 – 500 nM at a constant myristoyl-CoA concentration of 250 nM. The data obtained were used to generate

initial rates of reaction from which K_M values were obtained using the GraFit software package (version 5.0.13, Erithacus Software, UK: www.erithacus.com/grafit/index.htm). The results quoted are the mean from triplicate assays.

Inhibition assay

Inhibitors, prepared as 100 mM stock solutions in DMSO, were diluted as required in assay buffer and used to replace the 25 μL buffer fraction in the standard SPA described above. Initially, inhibitors were screened at a single concentration (50 μM) to identify the compounds which produced the most effective inhibition of the target NMT. These were then further evaluated by determination of IC_{50} values. Inhibitor concentrations were varied from 100 nM - 1 mM at a constant myristoyl-CoA concentration (125 nM). The resulting data were plotted using GraFit and IC_{50} values determined from a four-parameter fit. Each IC_{50} value reported is the mean obtained from triplicate assays.

Parasite culture and inhibitor testing

The asexual erythrocytic stages of *P. falciparum* 3D7 were cultured using a modification of the procedures of Trager and Jensen [36]. Parasites were cultured in RPMI1640 supplemented with 0.5% w/v albumax I (GibcoBRL), 2 mM L-glutamine, 25 mM HEPES, 24 mM $NaHCO_3$, 25 μg ml^{-1} gentamycin, 16 μg ml^{-1} hypoxanthine, 1.6 mg ml^{-1} glucose. Human erythrocytes were obtained from the National Blood Transfusion Service. Cultures were maintained at 37 ºC in a haemocrit of 0.5-1% and a gas mixture of 7% CO_2, 5% O_2 and 88% N_2. Tight synchronisation was achieved using the Percoll method [37]. Schizonts, isolated by centrifugation through 70% Percoll (1000 *g*, 11 min), were added to fresh erythrocytes for 1 h, to allow invasion to occur, before removal of the residual schizonts by lysis with 5% w/v sorbitol in PBS. 70% Percoll was prepared by mixing Percoll 9:1 with 10 x PBS and mixing this 7:3 with RPMI 1640.

Selected compounds were added to the culture medium at a final concentration of 100 μM or 10 μM with 1% (v/v) DMSO. Inhibitor-free controls, both with and without 1% DMSO, were included. Experiments were initiated with three different stages of synchronised parasites at a parasitaemia of approximately 1%. Ring stage (*ca.* 5 h post invasion), trophozoite stage (ca. 27 h) and schizont stage (*ca.* 42 h) parasites were all allowed to develop, release and re-invade new red blood cells and progress to approximately 30 h in the next cycle. This resulted in a total inhibitor exposure time of 68, 53 and 31 h for the ring, trophozoite and schizont stages, respectively. At the end of each experiment, parasite morphology was examined and the numbers of infected RBCs were determined by Giemsa staining and light microscopy, counting > 2000 red blood cells per sample. The results shown are the mean of a triplicate repeat.

RESULTS and DISCUSSION

Codon optimisation improves the yield of PfNMT

In an attempt to improve heterologous expression of PfNMT in *E. coli*, codon optimisation of *PfNMT* was undertaken to remove codons rarely used in *E. coli*. These changes also resulted in an overall reduction in AT content from 73% to 60% (see supplementary figure). Expression of soluble, active protein was achieved by creating an expression construct in which the optimised *PfNMT* coding sequence was cloned into the *Bam*H1 and *Eco*R1 restriction sites of the pTrcHisA expression vector. High levels of PfNMT overexpression were also observed using pET 28a and pGEX 5X-1 expression vectors but in these cases, the proteins remained insoluble (data not shown).

A three-stage protein purification strategy was developed. Purification of PfNMT from *E. coli* lysates by IMAC using Ni Sepharose was the preferred method for the capture stage of the purification. This resin is tolerant to low concentrations of DTT, which was found to reduce precipitation of PfNMT on storage. Mutation of Cys228 to Ser was also observed to reduce precipitation of purified PfNMT (PWB, unpublished observations). However, as Cys228 is predicted to reside at the bottom of the peptide-binding pocket (based upon comparisons with other known NMT structures), all subsequent work was carried out with purified recombinant wild-type enzyme stabilised with DTT rather than the C228S mutant (which has the potential to alter substrate binding).

Sequential stages in the purification of PfNMT are shown in Figure 1. PfNMT is the major band following capture with Ni-Sepharose IMAC (Lane 1, apparent molecular mass ~50 kDa, consistent with predictions from primary sequence analysis). Concentration of this material and subsequent separation by size exclusion chromatography yielded a fraction containing PfNMT with a retention time consistent with a monomeric form of the enzyme. This fraction also contained some contaminating species with lower molecular masses (lane 2). In the absence of DTT, a second peak with a retention time consistent with a 75 kDa protein complex was also observed; this peak was eliminated in the presence of 5 mM DTT (data not shown). The final stage of the purification used cation-exchange chromatography (see Methods) and resulted in the separation of PfNMT from all but one significant impurity (Lane 3). This was identified, by peptide mass fingerprinting, as an *E. coli* Cap-DNA recognition protein with a predicted mass of 24 kDa. The protein band observed at 50 kDa was confirmed as PfNMT by peptide mass fingerprinting with > 60% peptide coverage. The overall yield was typically 400 $\mu g\ L^{-1}$ representing a >20-fold improvement on previous methods [28]. Glycerol was added to a final concentration of 25% (v/v) in the PfNMT sample which was then stored at -20 ºC. When stored in this way PfNMT remained stable for > 2 years with negligible loss in activity (as tested in the SPA). Storage at 4 ºC resulted in formation of a precipitate and loss of activity; this precipitation was decreased, but not eliminated, in the C228S variant.

Codon optimisation and the creation of synthetic *P. falciparum* genes have been shown to be an effective strategy for improving expression efficiency in heterologous expression systems such as *P. pastoris* [38], baculovirus [39], murine cells [40] and *E. coli* [41]. However, in a recent extensive study investigating ~1000 *P. falciparum* open reading frames in an *E. coli* expression system [42], only a fraction of the selected sequences were successfully expressed (337, of which only 63 provided significant levels of soluble protein). Further investigation of sequences with little or no expression was conducted using alternative expression approaches and revealed little advantage to codon optimisation (3 out of 12 gave insoluble protein) and insect cell expression systems (1 out of 17 proteins previously obtained in the insoluble fraction gave soluble protein). Although some success was obtained with each of these alternatives, no ideal system for expression of *P. falciparum* proteins could be determined. Most recently Vedadi et al. [43] have reported the effective use of an *E. coli* expression platform to obtain structural information for apicomplexan proteins by attempting expression of ~400 *P. falciparum* genes along with selected orthologues. The differing expression profiles of orthologous proteins in the *E. coli* system resulted in successful structural determinations for significantly increased numbers of the target proteins or their orthologues. Expression studies have not been conducted on other apicomplexan NMTs to date. In this study, we have concentrated on the *P. falciparum* NMT and demonstrated the benefits of codon optimisation for soluble protein expression from this particular gene.

Development of a scintillation proximity assay for NMT activity

The *N*-myristoylation reaction transfers myristate from myristoyl-CoA to the N-terminus of a peptide/protein substrate. The majority of the assays developed for monitoring NMT activity have used radiolabel transfer to achieve high sensitivity with subsequent separation of product by HPLC or binding to phosphocellulose paper [27, 44, 45]. Whilst these can be successfully used to monitor inhibition of NMT, we favoured an approach more suited to high throughput screening and later automation. For this purpose, we elected to use a scintillation proximity assay (SPA). The success of such an assay relies on incorporation of radiolabel into a product that can be selectively bound to the immobilised scintillant. In the case of *N*-myristoylation, ^{3}H-myristate is transferred to a biotinylated peptide substrate that is bound to streptavidin-coated scintillant beads after termination of the enzymatic reaction. The presence of the scintillant in the bead eliminates the liquid handling stages required by the most similar assay reported [26] which uses streptavidin-coated 96-well plates to isolate the ^{3}H-labelled peptide product before washing, to remove unreacted ^{3}H-myristate, and addition of a liquid scintillant to facilitate counting.

Choice of a suitable NMT substrate was critical for successful assay development. We have previously shown that recombinant *P. falciparum* ADP ribosylation factor 1 (PfARF1) is a PfNMT substrate both *in vitro* and *in vivo* [28, 29], while reconstituted *N*-myristoylation assays in *E. coli* have demonstrated that PfARF1 is also a substrate for CaNMT and HsNMT1 (data not shown).

On the basis of this information, two biotinylated peptides (PfARFshort and PfARFlong, Table 1) were synthesized (by SPPS) for use as artificial PfNMT substrates. PfARFshort and PfARFlong contain residues 2-15 or 2-16, respectively, of PfARF1 (omitting the N-terminal initiator methionine). Both peptides also contain a biotinylated lysine replacing the naturally occurring lysine as the C-terminal residue. These longer peptides were used in preference to the octapeptides used in many NMT substrate studies [46-48], to prevent the C-terminal biotinylated lysine from interacting with the peptide binding pocket, thereby minimising potential steric hindrance which could adversely affect the *N*-myristoylation reaction. Both peptides were confirmed as PfNMT substrates in an HPLC-based activity assay (data not shown). PfARFlong was demonstrated as the better SPA substrate in the same HPLC assay and subsequently in K_M determinations using the SPA (K_M 1.2 μM ± 0.4 vs 7.1 μM ± 1.3 for PfARFshort).

Development of the SPA was therefore initiated using the PfARFlong substrate (Figure 2). First, the dependence of radioactive incorporation on the presence of both enzyme and peptide substrate was confirmed (Figure 2A). Substituting PfARFlong with AlaARF (in which the N-terminal glycine is replaced by alanine; Table 1) resulted in no detectable signal over background levels. This is consistent with published fungal NMT data, demonstrating that an N-terminal glycine residue is required for enzymatic *N*-myristoylation [48]. The SPA format also requires discontinuous sampling, taking single time point measurements for each reaction condition and enzyme tested. In order to determine the rate limiting concentrations of NMT required for constant reaction rate over a standard period (allowing initial rate determinations), increasing concentrations of CaNMT, HsNMT and PfNMT were titrated over a 30 min reaction (Figure 2B). A peptide concentration was selected to allow total binding to the scintillant beads, thus eliminating competition for binding sites between unreacted biotinylated substrate and *N*-myristoylated product. It is possible to use larger quantities of biotinylated peptide in the reaction (greater than the bead capacity), but the decreased signal resulting from the competitive binding and the additional error dependent on SPA bead concentration made this approach less favourable. The bead capacity for PfARFlong was found to be 50-100 pmol mg^{-1}.

To further validate the optimised SPA conditions developed above, CaNMT and a known inhibitor of its activity, UK362091 (Pfizer), were used in an IC_{50} determination (Figure 2C). The IC_{50} value recorded (11.6 ± 1.5 nM) is consistent with that previously determined at Pfizer (19 nM, unpublished data). In addition, we have previously reported the favourable comparison of the SPA with a more laborious phosphocellulose paper binding assay, using TbNMT and a biotinylated substrate based on the *T. brucei* CAP5.5 protein [27]. In view of these collective results, the optimised SPA methods could now be applied to the screening of fungal NMT inhibitors against PfNMT and HsNMT1 in a 96-well plate format.

Inhibitors based around a benzothiazole scaffold can inhibit PfNMT in vitro

Initial screening for inhibition of PfNMT was conducted using five of the fungal NMT inhibitors described previously in studies on TbNMT and LmNMT [27]. Compounds CP005240 and CP014553, identified as inhibitors of TbNMT, were also identified as the most potent inhibitors of PfNMT *in vitro* (IC_{50} values of 360 nM and 280 nM respectively, Table 2). However, in contrast to TbNMT, relative inhibition (as compared with HsNMT1) was also achieved with UK370485. Forty-three compounds (provided by Pfizer), each containing the same benzothiazole scaffold as UK370485, were screened for inhibitory activity at 50 μM against both PfNMT and HsNMT1. Seven compounds showed >25% inhibitory activity against recombinant PfNMT (data not shown). IC_{50} values were generated for these, together with four non-benzothiazoles, previously analysed against LmNMT and TbNMT [27] (labelled * in Table 2). Table 2 shows that three benzothiazole-containing compounds (1, 4 and 7) have IC_{50} values < 50 μM for PfNMT. All the compounds shown in Table 2 showed some selectivity for PfNMT, with the exception of compound 2 (UK370710) which is more inhibitory to HsNMT than PfNMT.

The structures of these active benzothiazole compounds are shown in Figure 3. Comparison reveals that the cyclohexyl linker region between the benzothiazole functionality and the aromatic group contains two distinct regiochemistries: 1,4-substituted (compounds 1-3), and (*R,S)* 1,3-substituted (compounds 4-7) in contrast to the starting compound UK370485, which is *trans*-1,4. The effect of modifications at the C-6 position of the benzothiazole group can be seen in the reversal of selectivity between PfNMT and HsNMT1 upon change from small fluorine or hydrogen atoms (compounds 3 and 1) to the bulky pyridin-2-yl functionality (compound 2). The majority of compounds that showed inhibition of PfNMT contain the dimethylamide group that is known to form favourable binding interactions in the peptide-binding pocket of CaNMT (Pfizer). Optimisation of both the C-6 substitution and the linker region is currently in progress and presents an opportunity to increase specificity and selectivity of the inhibitors.

Benzothiazole based inhibitors are toxic to cultured asexual stages of *P. falciparum*

Compounds 1, 3, 4 and 7 (Figure 3 and Table 2) were applied at concentrations of 100 μM and 10 μM to synchronised trophozoite stage *P. falciparum* 3D7 (approximately 27 h post invasion). Figure 4 shows the effect of these compounds on total parasitaemia, compared to controls containing 1% DMSO (v/v) only. In all cases, there is a significant reduction in parasitaemia at 100 μM to a level similar to the starting parasitaemia (ca. 1%). In the case of compounds 1 and 3 at 10 μM, there is approximately an 80% reduction in parasitaemia compared to the controls with DMSO only (t-test, $P < 0.03$). This inhibitory effect is greater than that observed for compounds CP005240 and CP014553, despite the higher IC50s of the benzothiazoles in the SPA (Table 2).

Changes in parasite morphology were also monitored following the application of different compound concentrations at three different start-points (5 h, 27 h and 42 h post invasion), followed by continuous culture until the mid-trophozoite stage (for controls) in the next cycle (data not shown). In all samples treated with potent compounds, a short survival time was indicated by the presence of dead or dying parasites (as assessed by abnormal morphology) that progressed only a short distance through the life-cycle. However, these dead or dying parasites were infrequent; instead, the large reduction in parasitaemia between experimental samples and controls resulted from the complete absence of detectable Giemsa-stained parasites, suggesting that these cells degenerate quickly and are incapable of invasion and development. Some parasites that did not die in the strongly-inhibited samples were characterised by considerably slower development, with parasites still at the ring stage when control cultures were at the trophozoite stage (> 10 h delay over a 48 h time course; data not shown). In the cultures treated with10 μM of compounds 1 and 3, the effect on both reduction in parasitaemia and delay in development was reduced, although not significantly. Parasites grown in the presence of 10 μM of compounds 4 and 7 were indistinguishable from the controls. The reasons for the striking differences in morphology observed between compounds 1, 3 and 4, 7 are not known but may be due to different levels of uptake and accumulation by the cultured cells. Additional off-target effects of these compounds, distinct from their inhibitory role against PfNMT, cannot be discounted at this stage.

Outlook

Previous investigations into parasitic protozoan NMT inhibitors have focused on a "piggy-back" approach, using compounds originally identified as NMT inhibitors for the fungal pathogens, *C. albicans* and *Aspergillus fumigatus* [11, 27]. We have also reported a small-scale study using peptide aptamers for inhibition of PfNMT [49]. The piggy-back screening approaches for PfNMT reported here have identified a benzothiazole-based compound that shows anti-parasitic activity in culture, prompting testing of a range of structurally related compounds. This has led to the identification of several structurally-related compounds with IC_{50} values < 50 μM, that show some selectivity over HsNMT1 and anti-parasitic activity against cultured *P. falciparum*. These results compare favourably with those obtained for the highest affinity inhibitors identified in screens of HsNMT1 by French et al. [26], using a library of 14,000 compounds. Notably, one compound, containing the benzothiazole scaffold, was also found to have an IC_{50} < 50 μM against HsNMT1, demonstrating the value of this piggy-back experimental approach in rapidly identifying drug-like molecules with a potential for further development to provide inhibitors of both HsNMT and PfNMT.

The compounds reported here represent the first evidence of a related family of molecules capable of inhibiting PfNMT. All these compounds were originally synthesised as part of an investigation into inhibitors of fungal NMTs and the discovery of compounds with high

affinity for PfNMT was not presumed. The success of this piggy-back approach in discovering one family of molecules suggests that further compound optimisation and validation of PfNMT as an anti-malarial target can be undertaken. Furthermore, the high-throughput screening capacity of the SPA developed as part of these studies not only creates opportunities expanding research efforts to develop an effective inhibitor of PfNMT, but can also be applied to other NMTs from different sources of therapeutic interest.

We thank Tanya Parkinson, Andy Bell and colleagues at Pfizer for technical advice and helpful discussions. This work was funded by the Wellcome Trust (061343, programme grant to DFS; 065514, studentship to PWB) and the U.K. Medical Research Council.

FIGURE LEGENDS

Figure 1 Purification of recombinant PfNMT

Recombinant PfNMT was enriched in three stages from *E. coli* soluble lysate, prepared following protein expression in a 50 L fermenter. Products after pooling of fractions showing NMT activity from each purification stage were separated by SDS-PAGE as shown. Lane 1 – Capture stage using Ni-Sepharose IMAC. Lane 2 – Intermediate purification on Sephacryl S-100 size exclusion column. Lane 3 – Final stage using ReSourceS cation exchange (pooled active NMT fractions shown). M, molecular mass markers. In Lane 3, the band migrating at approximately 50 kDa (+) was identified as PfNMT by peptide mass fingerprinting. The major impurity (*) was characterized by peptide mass fingerprinting and is most likely to be an *E. coli* Cap-DNA Recognition protein (gi:2098303), consistent with the observed molecular mass of 24 kDa.

Figure 2 Development of SPA for NMT activity

A. The SPA was conducted with 500 nM PfARFlong substrate, 500 nM myristoyl CoA and 100ng PfNMT at 37 ºC. Sampling was conducted at five different timepoints (0, 40, 90, 150 and 240 min) to monitor reaction progression. Four different samples were used in a typical reaction timecourse (filled triangles): a reaction with no peptide (open circles), no NMT (filled circles), and AlaARF peptide replacing peptide substrate (open squares).

B. The concentration of NMT was titrated by serial dilution in otherwise identical reactions incubated for 30 min using 125 nM ARFlong peptide and 125 nM myristoyl-CoA, in a final volume of 100 µL. Enzyme concentration, as a percentage of the highest concentration used, is plotted against cpm for reactions using CaNMT (open triangles), PfNMT (filled squares) and HsNMT1 (open circles). A close approximation to a linear fit demonstrates that enzyme concentrations can be selected so that the amount of enzyme is rate limiting under the experimental conditions selected. A.u., arbitrary units.

C. An IC_{50} value for inhibitor UK 362091 with CaNMT was determined using the SPA. Inhibitor concentrations were varied from 1 µM - 42 pM in otherwise identical reactions (125 nM PfARFlong peptide, 125 nM myristoyl-CoA, 3 ng CaNMT). A plot of cpm, after 30 min incubation at 37 ºC, against inhibitor concentration allows a four-parameter fit to derive the point at which the signal is half maximal, the IC_{50}. The error bars are the standard deviation around the mean from a triplicate repeat. The IC_{50} value obtained is 11.6 nM (see inset), consistent with a previous evaluation of 19 nM (Pfizer, unpublished data).

Figure 3 Structures of PfNMT inhibitors based around a benzothiazole core structure

Structures of the seven compounds which demonstrated the highest levels of PfNMT inhibition are shown below, together with the parent compound, UK370485. All compounds contain a benzothiazole core. Compounds 1-3 are identical, apart from the C-6 substitution on the benzothiazole ring. Compounds 4-7 are more diverse in structure but all contain a cyclohexyl linker with 1R, 3S stereochemistry (as opposed to 1S, 4S in compounds 1-3) and a dimethylamide as the C-6 benzothiazole substituent.

Figure 4 Inhibitors of PfNMT in vitro reduce *P. falciparum* parasitaemia in culture

Each inhibitor was applied to synchronised mid-trophozoite erythrocytic stages of *P. falciparum* (27 h) at 100 μM and 10 μM and the culture was allowed to grow until controls had reached a similar stage in the following cycle (approximately 48 h later). The total parasitaemia of each sample was evaluated by microscopic assessment of Giesma-stained blood smears. Error bars are the standard deviation around the mean for a triplicate repeat. All experiments were initiated at a parasitaemia of approximately 1%.

Table 1 Peptides evaluated as substrates of PfNMT

The peptides listed were synthesised by standard Fmoc ^{t}Bu SPPS from Rink-Amide MBHA resin pre-loaded with biotinylated lysine, giving a C-terminal amide and glycine or alanine as the N-terminal residue. ARF peptides are based on the N-terminal sequence of PfARF1. K_M values for the substrate peptides demonstrate that ARFlong is a better substrate than ARFshort. Peptides with Ala replacing Gly are not substrates for PfNMT.

Peptide Sequence	Name	K_M (μM)
GLYVSRLFNRLFQKK(Biotin)-NH_2	ARFlong	1.2 ± 0.4
GLYVSRLFNRLFQK(Biotin)-NH_2	ARFshort	7.1 ± 1.0
GSQGSKPVDTSDVK(Biotin)-NH_2	PfEMP	Not a substrate
ALYVSRLFNRLFQKK(Biotin)- NH_2	AlaARFlong	Not a substrate
ALYVSRLFNRLFQK(Biotin)- NH_2	AlaARFshort	Not a substrate

Table 2 IC_{50} values for benzothiazole inhibitors showing activity at 50 μM

IC_{50} values were determined using the SPA as described for PfNMT and HsNMT1. Compounds previously evaluated as inhibitors of TbNMT and LmNMT (*; [27]) were investigated together with benzothiazole-based inhibitors (structures 1-7 in Figure 3) that show inhibitory activity at 50 μM.

Inhibitor	IC_{50} value determined in SPA (μM)	
	PfNMT	HsNMT
CP 005240 (*)	0.36 +/- 0.04	1.8 +/- 0.3
CP 014553 (*)	0.28 +/- 0.12	1.6 +/- 0.5
CP 144568 (*)	300 +/- 78	>1000
UK 370485 (*)	232 +/- 46	>1000
UK 145974 (*)	> 1000	>1000
UK370309 (4)	17 ± 1	331 ± 29
UK370509 (1)	30 ± 3	286 ± 93
UK370624 (5)	53 ± 5	656 ± 210
UK370709 (6)	111 ± 7	711 ± 133
UK370710 (2)	115 ± 9	28 ± 9
UK362799 (3)	68 ± 4	309 ± 58
UK370713 (7)	37 ± 4	329 ± 84

REFERENCES

1 Snow, R. W., Guerra, C. A., Noor, A. M., Myint, H. Y. and Hay, S. I. (2005) The global distribution of clinical episodes of Plasmodium falciparum malaria. Nature **434**, 214-217

2 Wilcox, C., Hu, J. S. and Olson, E. N. (1987) Acylation of proteins with myristic acid occurs cotranslationally. Science **238**, 1275-1278

3 Resh, M. D. (1999) Fatty acylation of proteins: new insights into membrane targeting of myristoylated and palmitoylated proteins. Biochim. Biophys. Acta. **1451**, 1-16

4 Maurer-Stroh, S., Eisenhaber, B. and Eisenhaber, F. (2002) N-terminal N-myristoylation of proteins: refinement of the sequence motif and its taxon-specific differences. J. Mol. Biol. **317**, 523-540.

5 Maurer-Stroh, S. and Eisenhaber, F. (2004) Myristoylation of viral and bacterial proteins. Trends Microbiol. **12**, 178-185

6 Rudnick, D. A., McWherter, C. A., Rocque, W. J., Lennon, P. J., Getman, D. P. and Gordon, J. I. (1991) Kinetic and structural evidence for a sequential ordered Bi Bi mechanism of catalysis by Saccharomyces cerevisiae myristoyl-CoA:protein N-myristoyltransferase. J. Biol. Chem. **266**, 9732-9739

7 Farazi, T. A., Waksman, G. and Gordon, J. I. (2001) Structures of Saccharomyces cerevisiae N-myristoyltransferase with bound myristoylCoA and peptide provide insights about substrate recognition and catalysis. Biochemistry **40**, 6335-6343

8 Sogabe, S., Masubuchi, M., Sakata, K., Fukami, T. A., Morikami, K., Shiratori, Y., Ebiike, H., Kawasaki, K., Aoki, Y., Shimma, N., D'Arcy, A., Winkler, F. K., Banner, D. W. and Ohtsuka, T. (2002) Crystal Structures of Candida albicans N-Myristoyltransferase with Two Distinct Inhibitors. Chem. Biol. **9**, 1119-1128.

9 Sikorski, J. A., Devadas, B., Zupec, M. E., Freeman, S. K., Brown, D. L., Lu, H. F., Nagarajan, S., Mehta, P. P., Wade, A. C., Kishore, N. S., Bryant, M. L., Getman, D. P., McWherter, C. A. and Gordon, J. I. (1997) Selective peptidic and peptidomimetic inhibitors of Candida albicans myristoylCoA: protein N-myristoyltransferase: a new approach to antifungal therapy. Biopolymers **43**, 43-71

10 Georgopapadakou, N. H. (2002) Antifungals targeted to protein modification: focus on protein N-myristoyltransferase. Expert Opin. Investig. Drugs **11**, 1117-1125

11 Gelb, M. H., Van Voorhis, W. C., Buckner, F. S., Yokoyama, K., Eastman, R., Carpenter, E. P., Panethymitaki, C., Brown, K. A. and Smith, D. F. (2003) Protein farnesyl and N-myristoyl transferases: piggy-back medicinal chemistry targets for the development of antitrypanosomatid and antimalarial therapeutics. Mol. Biochem. Parasitol. **126**, 155-163

12 Selvakumar, P., Pasha, M. K., Ashakumary, L., Dimmock, J. R. and Sharma, R. K. (2002) Myristoyl-CoA:protein N-myristoyltransferase: a novel molecular approach for cancer therapy (Review). Int. J. Mol. Med. **10**, 493-500

13 Ducker, C. E., Upson, J. J., French, K. J. and Smith, C. D. (2005) Two N-myristoyltransferase isozymes play unique roles in protein myristoylation, proliferation, and apoptosis. Mol. Cancer Res. **3**, 463-476

14 Selvakumar, P., Lakshmikuttyamma, A., Shrivastav, A., Das, S. B., Dimmock, J. R. and Sharma, R. K. (2007) Potential role of N-myristoyltransferase in cancer. Prog. Lipid Res. **46**, 1-36. Epub 2006 Jun 2012.

15 Selvakumar, P., Smith-Windsor, E., Bonham, K. and Sharma, R. K. (2006) N-myristoyltransferase 2 expression in human colon cancer: cross-talk between the calpain and caspase system. FEBS Lett. **580**, 2021-2026. Epub 2006 Mar 2027.

16 Lodge, J. K., Jackson-Machelski, E., Toffaletti, D. L., Perfect, J. R. and Gordon, J. I. (1994) Targeted gene replacement demonstrates that myristoyl-CoA: protein N-myristoyltransferase is essential for viability of Cryptococcus neoformans. Proc. Natl. Acad. Sci. U S A **91**, 12008-12012

17 Weinberg, R. A., McWherter, C. A., Freeman, S. K., Wood, D. C., Gordon, J. I. and Lee, S. C. (1995) Genetic studies reveal that myristoylCoA:protein N-myristoyltransferase is an essential enzyme in Candida albicans. Mol. Microbiol. **16**, 241-250

18 Price, H. P., Menon, M. R., Panethymitaki, C., Goulding, D., McKean, P. G. and Smith, D. F. (2003) Myristoyl-CoA:protein N-myristoyltransferase, an essential enzyme and potential drug target in kinetoplastid parasites. J. Biol. Chem. **278**, 7206-7214

19 Kishore, N. S., Wood, D. C., Mehta, P. P., Wade, A. C., Lu, T., Gokel, G. W. and Gordon, J. I. (1993) Comparison of the acyl chain specificities of human myristoyl-CoA synthetase and human myristoyl-CoA:protein N-myristoyltransferase. J. Biol. Chem. **268**, 4889-4902

20 Cordo, S. M., Candurra, N. A. and Damonte, E. B. (1999) Myristic acid analogs are inhibitors of Junin virus replication. Microbes Infect. **1**, 609-614

21 Devadas, B., Freeman, S. K., McWherter, C. A., Kishore, N. S., Lodge, J. K., Jackson-Machelski, E., Gordon, J. I. and Sikorski, J. A. (1998) Novel biologically active nonpeptidic inhibitors of myristoylCoA:protein N-myristoyltransferase. J. Med. Chem. **41**, 996-1000

22 Yamazaki, K., Kaneko, Y., Suwa, K., Ebara, S., Nakazawa, K. and Yasuno, K. (2005) Synthesis of potent and selective inhibitors of Candida albicans N-myristoyltransferase based on the benzothiazole structure. Bioorg. Med. Chem. **13**, 2509-2522

23 Ebiike, H., Masubuchi, M., Liu, P., Kawasaki, K., Morikami, K., Sogabe, S., Hayase, M., Fujii, T., Sakata, K., Shindoh, H., Shiratori, Y., Aoki, Y., Ohtsuka, T. and Shimma, N. (2002) Design and synthesis of novel benzofurans as a new class of antifungal agents targeting fungal N-myristoyltransferase. Part 2. Bioorg. Med. Chem. Lett. **12**, 607-610

24 Duronio, R. J., Reed, S. I. and Gordon, J. I. (1992) Mutations of human myristoyl-CoA:protein N-myristoyltransferase cause temperature-sensitive myristic acid auxotrophy in Saccharomyces cerevisiae. Proc. Natl. Acad. Sci. U S A **89**, 4129-4133

25 Giang, D. K. and Cravatt, B. F. (1998) A second mammalian N-myristoyltransferase. J. Biol. Chem. **273**, 6595-6598

26 French, K. J., Zhuang, Y., Schrecengost, R. S., Copper, J. E., Xia, Z. and Smith, C. D. (2004) Cyclohexyl-octahydro-pyrrolo[1,2-a]pyrazine-based inhibitors of human N-myristoyltransferase-1. J. Pharmacol. Exp. Ther. **309**, 340-347

27 Panethymitaki, C., Bowyer, P. W., Price, H. P., Leatherbarrow, R. J., Brown, K. A. and Smith, D. F. (2006) Characterisation and selective inhibition of Myristoyl CoA: protein N-myristoyl transferase from Trypanosoma brucei and Leishmania major. Biochem. J.

28 Gunaratne, R. S., Sajid, M., Ling, I. T., Tripathi, R., Pachebat, J. A. and Holder, A. A. (2000) Characterization of N-myristoyltransferase from Plasmodium falciparum. Biochem. J. **348 Pt 2**, 459-463

29 Rees-Channer, R. R., Martin, S. R., Green, J. L., Bowyer, P. W., Grainger, M., Molloy, J. E. and Holder, A. A. (2006) Dual acylation of the 45 kDa gliding-associated protein (GAP45) in Plasmodium falciparum merozoites. Mol. Biochem. Parasitol. **149**, 113-116

30 Struck, N. S., de Souza Dias, S., Langer, C., Marti, M., Pearce, J. A., Cowman, A. F. and Gilberger, T. W. (2005) Re-defining the Golgi complex in Plasmodium falciparum using the novel Golgi marker PfGRASP. J. Cell. Sci. **118**, 5603-5613

31 Moskes, C., Burghaus, P. A., Wernli, B., Sauder, U., Durrenberger, M. and Kappes, B. (2004) Export of Plasmodium falciparum calcium-dependent protein kinase 1 to the parasitophorous vacuole is dependent on three N-terminal membrane anchor motifs. Mol. Microbiol. **54**, 676-691

32 Bowyer, P. W. (2007) Studies on the N-myristoyltransferase of Plasmodium falciparum. PhD Thesis, University of London

33 Hale, R. S. and Thompson, G. (1998) Codon optimization of the gene encoding a domain from human type 1 neurofibromin protein results in a threefold improvement in expression level in Escherichia coli. Protein. Expr. Purif. **12**, 185-188.

34 Withers-Martinez, C., Carpenter, E. P., Hackett, F., Ely, B., Sajid, M., Grainger, M. and Blackman, M. J. (1999) PCR-based gene synthesis as an efficient approach for expression of the A+T-rich malaria genome. Protein Eng. **12**, 1113-1120.

35 Fields, G. B. and Noble, R. L. (1990) Solid phase peptide synthesis utilizing 9-fluorenylmethoxycarbonyl amino acids. Int. J. Pept. Protein Res. **35**, 161-214.

36 Trager, W. and Jensen, J. B. (1976) Human malaria parasites in continuous culture. Science **193**, 673-675

37 Pasvol, G., Wilson, R. J., Smalley, M. E. and Brown, J. (1978) Separation of viable schizont-infected red cells of Plasmodium falciparum from human blood. Ann. Trop. Med Parasitol. **72**, 87-88.

38 Kocken, C. H., Withers-Martinez, C., Dubbeld, M. A., van der Wel, A., Hackett, F., Valderrama, A., Blackman, M. J. and Thomas, A. W. (2002) High-level expression of the malaria blood-stage vaccine candidate Plasmodium falciparum apical membrane antigen 1 and induction of antibodies that inhibit erythrocyte invasion. Infect. Immun. **70**, 4471-4476

39 Withers-Martinez, C., Carpenter, E. P., Hackett, F., Ely, B., Sajid, M., Grainger, M. and Blackman, M. J. (1999) PCR-based gene synthesis as an efficient approach for expression of the A+T-rich malaria genome. Protein Eng. **12**, 1113-1120

40 Narum, D. L., Kumar, S., Rogers, W. O., Fuhrmann, S. R., Liang, H., Oakley, M., Taye, A., Sim, B. K. and Hoffman, S. L. (2001) Codon optimization of gene fragments encoding Plasmodium falciparum merzoite proteins enhances DNA vaccine protein expression and immunogenicity in mice. Infect. Immun. **69**, 7250-7253

41 Dutta, S., Lalitha, P. V., Ware, L. A., Barbosa, A., Moch, J. K., Vassell, M. A., Fileta, B. B., Kitov, S., Kolodny, N., Heppner, D. G., Haynes, J. D. and Lanar, D. E. (2002) Purification, characterization, and immunogenicity of the refolded ectodomain of the Plasmodium falciparum apical membrane antigen 1 expressed in Escherichia coli. Infect. Immun. **70**, 3101-3110

42 Mehlin, C., Boni, E., Buckner, F. S., Engel, L., Feist, T., Gelb, M. H., Haji, L., Kim, D., Liu, C., Mueller, N., Myler, P. J., Reddy, J. T., Sampson, J. N., Subramanian, E., Van Voorhis, W. C., Worthey, E., Zucker, F. and Hol, W. G. (2006) Heterologous expression of proteins from Plasmodium falciparum: results from 1000 genes. Mol. Biochem. Parasitol. **148**, 144-160

43 Vedadi, M., Lew, J., Artz, J., Amani, M., Zhao, Y., Dong, A., Wasney, G. A., Gao, M., Hills, T., Brokx, S., Qiu, W., Sharma, S., Diassiti, A., Alam, Z., Melone, M., Mulichak, A., Wernimont, A., Bray, J., Loppnau, P., Plotnikova, O., Newberry, K., Sundararajan, E., Houston, S., Walker, J., Tempel, W., Bochkarev, A., Kozieradzki, I., Edwards, A., Arrowsmith, C., Roos, D., Kain, K. and Hui, R. (2007) Genome-scale protein expression and structural biology of Plasmodium falciparum and related Apicomplexan organisms. Mol. Biochem. Parasitol. **151**, 100-110. Epub 2006 Nov 2013.

44 Glover, C. J., Goddard, C. and Felsted, R. L. (1988) N-myristoylation of p60src. Identification of a myristoyl-CoA:glycylpeptide N-myristoyltransferase in rat tissues. Biochem. J.**250**, 485-491

45 King, M. J. and Sharma, R. K. (1991) N-myristoyl transferase assay using phosphocellulose paper binding. Anal. Biochem. **199**, 149-153

46 McWherter, C. A., Rocque, W. J., Zupec, M. E., Freeman, S. K., Brown, D. L., Devadas, B., Getman, D. P., Sikorski, J. A. and Gordon, J. I. (1997) Scanning alanine mutagenesis and de-peptidization of a Candida albicans myristoyl-CoA:protein N-myristoyltransferase octapeptide substrate reveals three elements critical for molecular recognition. J. Biol. Chem. **272**, 11874-11880

47 Rocque, W. J., McWherter, C. A., Wood, D. C. and Gordon, J. I. (1993) A comparative analysis of the kinetic mechanism and peptide substrate specificity of human and Saccharomyces cerevisiae myristoyl-CoA:protein N-myristoyltransferase. J. Biol. Chem. **268**, 9964-9971

48 Towler, D. A., Eubanks, S. R., Towery, D. S., Adams, S. P. and Glaser, L. (1987) Amino-terminal processing of proteins by N-myristoylation. Substrate specificity of N-myristoyl transferase. J. Biol. Chem. **262**, 1030-1036

49 Tate, E. W., Bowyer, P. W., Brown, K. A., Smith, D. F., Holder, A. A. and Leatherbarrow, R. J. (2006) Peptide-based inhibitors of N-myristoyl transferase generated from a lipid/combinatorial peptide chimera library. Signal Transduction **6**, 160-166

Figure 1. Purification of recombinant PfNMT

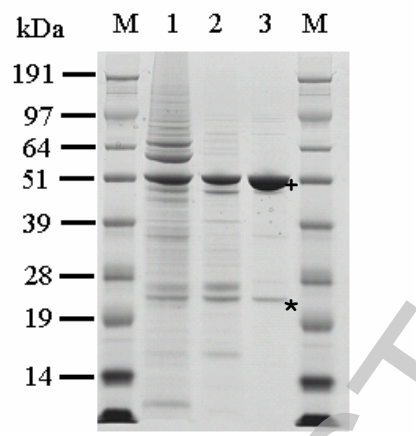

Figure 2. Development of SPA for NMT activity

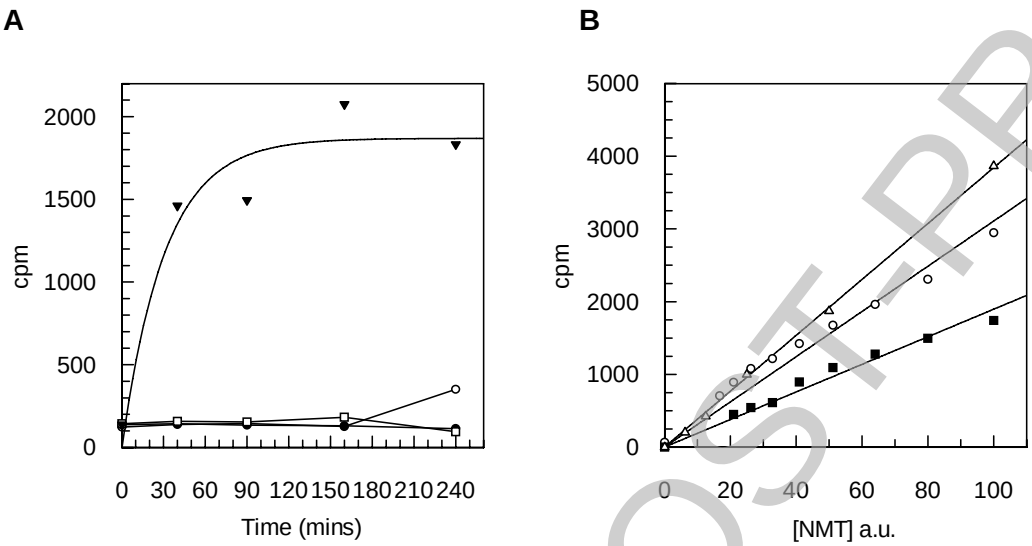

C

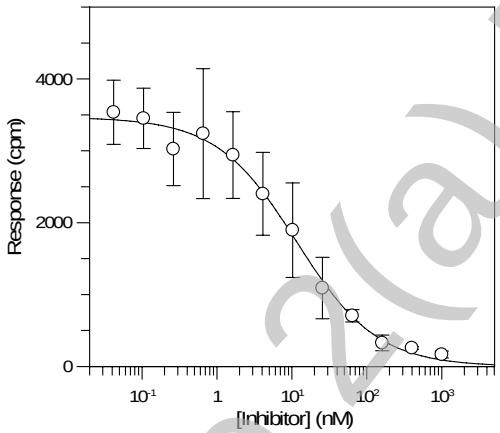

Parameter	Value	Std Error
Y Range (cpm)	3467.0	88.0
IC_{50} (nM)	11.6	1.5
Slope factor	0.8	0.1

Figure 3. Structures of PfNMT inhibitors based around a benzothiazole core structure

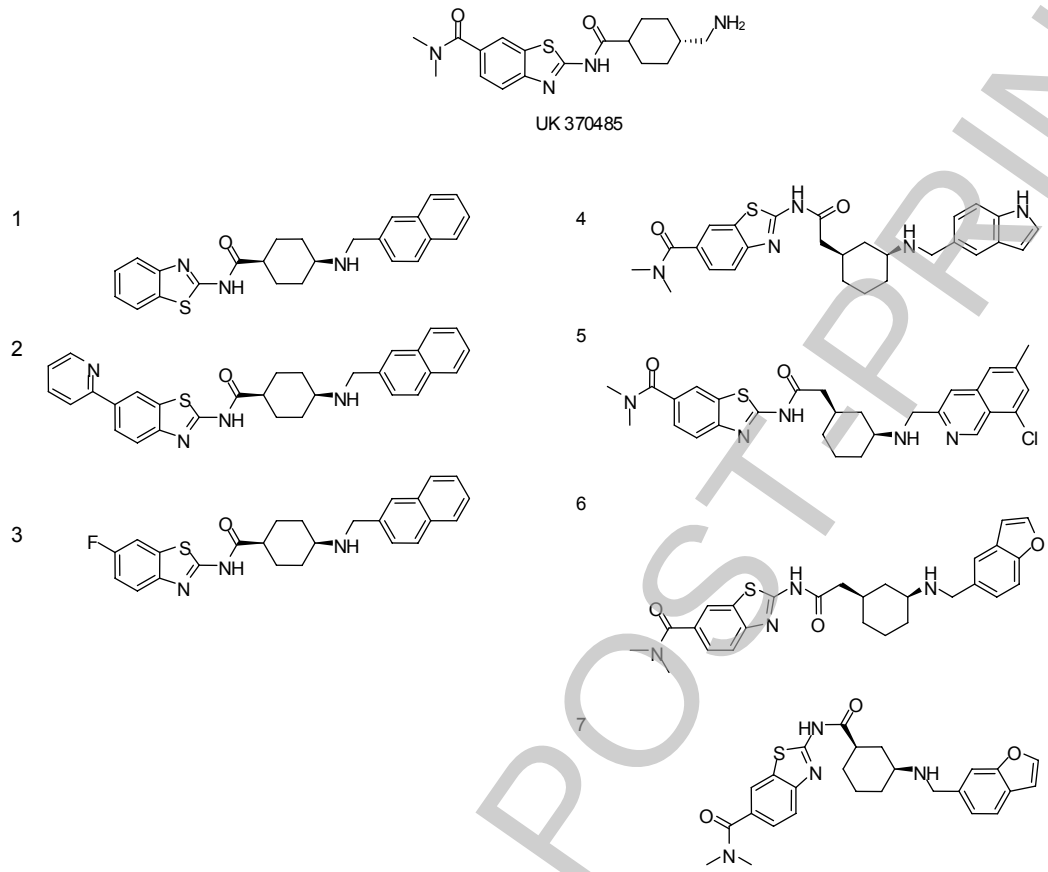

Biochemical Journal Immediate Publication. Published on 23 Aug 2007 as manuscript BJ20070692

Figure 4. Inhibitors of PfNMT in vitro reduce *P. falciparum* parasitaemia in culture

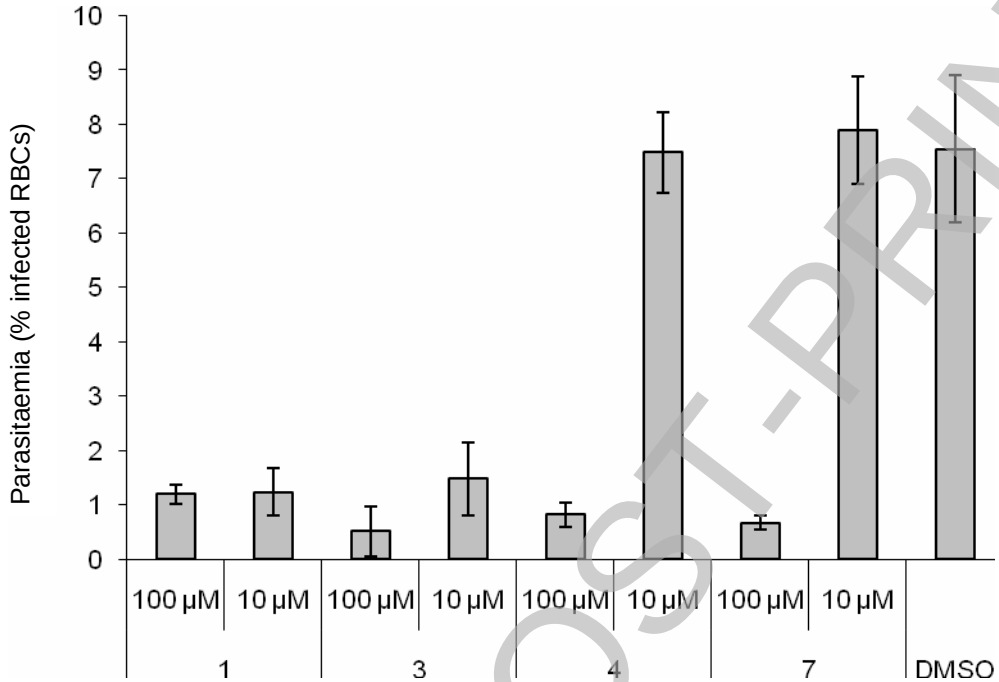

Inhibitor	Parasitaemia relative to control containing 1% v/v DMSO	
	100 µM Inhibitor	10 µM Inhibitor
1	15 ± 2	16 ± 6
3	7 ± 6	19 ± 9
4	11 ± 3	96 ± 10
7	9 ± 2	102 ±13